Experimental determination of the radial dose distribution in high gradient regions around ^{192}Ir wires: Comparison of electron paramagnetic resonance imaging, films, and Monte Carlo simulations

N. Kolbun and Ph. Levêque
Biomedical Magnetic Resonance Unit, Louvain Drug Research Institute, Université catholique de Louvain, Avenue Mounier 73.40, B-1200 Brussels, Belgium

F. Abboud, A. Bol, and S. Vynckier
Molecular Imaging and Experimental Radiotherapy Unit, Institute of Experimental and Clinical Research, Université catholique de Louvain, Avenue Hippocrate 55, B-1200 Brussels, Belgium

B. Gallez[a)]
Biomedical Magnetic Resonance Unit, Louvain Drug Research Institute, Université catholique de Louvain, Avenue Mounier 73.40, B-1200 Brussels, Belgium

(Received 22 February 2010; revised 7 August 2010; accepted for publication 17 August 2010; published 28 September 2010)

Purpose: The experimental determination of doses at proximal distances from radioactive sources is difficult because of the steepness of the dose gradient. The goal of this study was to determine the relative radial dose distribution for a low dose rate ^{192}Ir wire source using electron paramagnetic resonance imaging (EPRI) and to compare the results to those obtained using Gafchromic EBT film dosimetry and Monte Carlo (MC) simulations.
Methods: Lithium formate and ammonium formate were chosen as the EPR dosimetric materials and were used to form cylindrical phantoms. The dose distribution of the stable radiation-induced free radicals in the lithium formate and ammonium formate phantoms was assessed by EPRI. EBT films were also inserted inside in ammonium formate phantoms for comparison. MC simulation was performed using the MCNP4C2 software code.
Results: The radical signal in irradiated ammonium formate is contained in a single narrow EPR line, with an EPR peak-to-peak linewidth narrower than that of lithium formate (~0.64 and 1.4 mT, respectively). The spatial resolution of EPR images was enhanced by a factor of 2.3 using ammonium formate compared to lithium formate because its linewidth is about 0.75 mT narrower than that of lithium formate. The EPRI results were consistent to within 1% with those of Gafchromic EBT films and MC simulations at distances from 1.0 to 2.9 mm. The radial dose values obtained by EPRI were about 4% lower at distances from 2.9 to 4.0 mm than those determined by MC simulation and EBT film dosimetry.
Conclusions: Ammonium formate is a suitable material under certain conditions for use in brachytherapy dosimetry using EPRI. In this study, the authors demonstrated that the EPRI technique allows the estimation of the relative radial dose distribution at short distances for a ^{192}Ir wire source. [DOI: 10.1118/1.3488913]

Key words: EPR, EPR imaging, brachytherapy, dosimetry, ^{192}Ir, Gafchromic EBT films, Monte Carlo

I. INTRODUCTION

Platinum encapsulated 0.3 mm diameter ^{192}Ir wires have been widely used as interstitial sources in low dose rate (LDR) brachytherapy. Due to the steep dose gradient in the millimeter distance range, it is difficult to perform accurate dose measurements with a high spatial resolution. This limitation has stimulated research for improved 2D and 3D dosimetry techniques.[1] The guidelines for dosimetry of brachytherapy sources in the centimeter distance range are presented in a report published by the American Association of Physicists in Medicine (AAPM) Radiation Therapy Committee Task Group 43 and can be extended to the millimeter range using the report of the AAPM Task Group 60.[2–4] Analytical Monte Carlo (MC) calculations provide reliable data on dose distribution.[5–9] Dose distribution can also be measured using ionization chambers of different sizes or LiF thermoluminescence dosimeters.[10–12] Films offer a high spatial resolution in a single 2D plane and provide relative dose information and absolute dose measurements when appropriately calibrated.[13,14] Gafchromic EBT (EBT) films are becoming increasingly popular due to their advantageous properties: They are nearly tissue equivalent (the effective atomic number of EBT film is Z_{eff}=6.98, this value is close to the Z_{eff} of water, which is 7.3); they have very low energy dependency, with not more than 5% difference between MeV and keV photons,[15] and they can be used to record the incidence of radiation at closely spaced points simultaneously and close to the source.

Electron paramagnetic resonance (EPR) spectroscopy represents a powerful tool for qualitative and quantitative analysis of radiation-induced stable free radicals. Solid-state dosimetry by means of EPR spectroscopy, usually with the amino acid L-α-alanine as a dosimeter, has been shown to be accurate at high doses (kGy region).[16,17] EPR measurements using alanine as a dosimetric material is internationally recognized as a standard method for reliable dose measurements.[18] Despite its wide use in reference laboratories, alanine is not routinely used in clinic where ionization chambers and diode detectors are more often preferred.

Polycrystalline formates and dithionates have been proposed recently as new materials for EPR dosimetry because the irradiation produces a large yield of stable free radicals with a linear dose response. Moreover, these compounds give a single-lined EPR spectrum, resulting in a higher peak-to-peak value of the central line as compared to the complicated alanine spectra.[19–22] The radiation energy dependency of ammonium formate is low above ~80 keV.[22] While EPR dosimetry can determine the concentration of free radicals, which is a function of the absorbed dose in whole samples, the distribution of radicals along two dimensions can be visualized by electron paramagnetic resonance imaging (EPRI). The first attempt to use EPRI in dosimetry was performed using alanine irradiated with electrons from a 4 MeV linear accelerator.[23] Other 2D EPRI experiments have been performed using alanine dosimeters irradiated with a 10 MeV electron beam or 10 MeV gamma photons.[24] Alanine dosimeters irradiated with beta (β) particles with high doses (up to 6 kGy) have also been examined by EPRI.[25] More recently, the evaluation of the dose distribution was obtained using potassium dithionate dosimeters irradiated by C^{6+} and N^{7+} ions.[26]

In a previous study, we demonstrated for the first time that 2D EPRI could be useful to determine the dose distribution around brachytherapy seeds using lithium formate (LiFo) as a dosimetric material.[27] Although we demonstrated that this approach was feasible, we concluded that the spatial resolution of the method was hampered by the large EPR linewidth of the lithium formate. The spatial resolution, which is the ability to distinguish two points in space, depends on the magnetic field gradient, the EPR linewidth of the material, and the deconvolution processing.[28] To overcome this possible limitation, we chose to study ammonium formate (HCO_2NH_4, AmFo). The radical signal in irradiated ammonium formate is contained in a single narrow EPR line, with an EPR linewidth narrower than that of lithium formate (~0.64 and 1.4 mT, respectively). Although EPR spectroscopy is a well established technology used for dosimetry studies, EPR imaging is yet to be validated. In this validation process, we explore the performances of EPR imaging, which is not yet a quantitative technique, to study the relative distribution of dose around brachytherapy sources (LDR ^{192}Ir) using a better dosimetric material, ammonium formate, compared to the previously used lithium formate. In the second part of the study, we compare the experimental relative EPRI dose distribution profiles for short distances, from 1.0 to 4.0 mm from the center of the source, to a validated experimental method using Gafchromic EBT films and to a theoretical method using MC simulations performed using the MCNP4C2 software code.

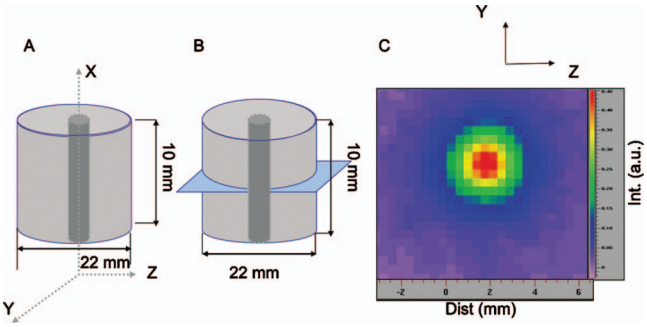

FIG. 1. Experimental setups used in the present study. (a) The setup for 2D EPR image reconstruction and the geometry used in the MC simulations. (b) The setup used for EBT film measurements and the geometry of the MC simulations including the film. (c) 2D reconstructed EPR image of the ammonium formate phantom irradiated by a ^{192}Ir wire source. Image directions relative to the EPR magnet are shown. Intensity integral is along the *X*-direction.

II. MATERIALS AND METHODS

II.A. Iridium wire sources

^{192}Ir wire source emits a spectrum of relatively low gamma energies with an average value of 360 keV; its half-life is 73.83 days.[6] The beta component of the ^{192}Ir spectrum has 180 keV average energy; however, the contribution of the beta particles was less than 0.01 (1%) even at the radial distance of r=0.5 mm.[9] Secondary electrons are also generated from platinum (Pt) encapsulation, but, at radial distances greater than about 1.0 mm, the dose rates including and excluding secondary electrons from the Pt encapsulation coincide with each other.[29,30]

The ^{192}Ir wire source (air kerma at 1 m: 2.52 μGy h^{-1} cm^{-1}, BEBIG GmbH, Berlin, Germany) had a length of 10.0 mm and a diameter of 0.3 mm. The central core was 0.1 mm in diameter, composed of about 20% Ir and 80% Pt, encased in a 0.1 mm Pt sheath. A radioactive wire was located at the center of the phantoms with its long axis coinciding with the phantom's central axis [cf. infra, EPR imaging section, and Fig. 1(a)].

II.B. Phantoms

The phantoms were made of polycrystalline lithium formate monohydrate or ammonium formate (Aldrich, Steinheim, Germany) powder pressed into small cylinders with a diameter of 22.0 mm and a height of 10.0 mm using a tablet press (Ateliers Courtoy, type AC27, Halle, Belgium, 50 kg/cm^2). For brachytherapy dosimetry, a hole (0.4 mm in diameter) was drilled at the center of all cylindrical phantoms. ^{192}Ir wires were inserted in the phantoms and were removed after 2 weeks of irradiation. Imaging was performed as soon as possible after the irradiation. As ammo-

nium formate is very hygroscopic, all samples were kept dry during the imaging process with a continuous flow of dry argon gas through the EPR cavity.

II.C. EPR Imaging

EPR spectra were collected using an L-band bridge Elexsys 540 spectrometer with a cylindrical cavity (ER 6502 BC, 25 mm in diameter) operating at 1.1 GHz and with 100 kHz magnetic field modulation. The signal intensity (measured as the peak-to-peak height) of the EPR spectra reflects the number of stable free radicals produced in the irradiated phantoms and provides a quantitative measurement of the absorbed dose.

2D EPR images were obtained using the same system. Planar (*ZY* plane) spatial images were acquired, where each pixel is the intensity integral of the spin density along the *x* dimension. The coordinate system has the longitudinal and transverse axes of the source as the *z* and *y* axes, respectively [Fig. 1(a)].

The applied magnetic field gradient was 450 mT/m and was generated by three orthogonal water-cooled cylindrical gradient coils. Other EPRI acquisition parameters were as follows: Applied modulation frequency of 100 kHz, microwave power of 28.6 or 57.6 mW, modulation amplitude of 0.25 mT, field of view of 25 mm, pixel size of 0.7 mm, and the number of pixels is 35. All imaging parameters were kept constant for all the irradiated phantoms.

II.C.1. Deconvolution: Image reconstruction

2D images were reconstructed on a 128×128 matrix by filtered backprojection using a Shepp–Logan filter. Before reconstruction, each projection was deconvolved using fast Fourier transform with the measured zero-gradient spectrum in order to improve image resolution.[31–34] To reduce noise amplification and avoid possible division by zero at high frequencies, a low pass filter was used. The deconvolution parameters, including the maximum cut-off frequency and the width of the window in the Fourier space, were set up after viewing the shape of all projections. Data were smoothed using either a Fermi–Dirac or a Gaussian filter. Spectral deconvolution and filtered backprojection were performed using the XEPR software package (Bruker GmbH, Rheinstetten, Germany).

Three 2D EPRI data sets were collected for each phantom and used to numerically analyze the relative radial dose distributions. All the relative radiation doses were doses to ammonium formate since ammonium formate was chosen as the reference material in this work. The dose measurements were made across the radial line profile from the center of the tablet in 0.35 mm steps. When the signal-to-noise ratio was greater than 2, the measured signal intensity was considered to be significant. The noise was measured in regions outside the area of the phantoms of 22 mm in diameter, where there were no signal sources.

The radial intensity profile extracted from each image was normalized to 100% at 1 mm from the center of the source as for other dosimetric methods. The results are given as the mean of three independent measurements.

II.D. EPRI resolution: Determination of the edge spread function

The theoretical spatial resolution, which represents the shortest distance (d) between two points that can be resolved in an EPR image, was calculated as follows:

$$d = \mathrm{LW}/G, \tag{1}$$

where LW (mT) is the linewidth of an EPR signal and G (mT/m) is the magnitude of the magnetic field gradient. The linewidths of the signal were 1.4 mT (LiFo) and 0.64 mT (AmFo), the magnetic field gradient was 450 mT/m, and the theoretical spatial resolutions were calculated as 3.1 and 1.4 mm, respectively.

The spatial resolution was also experimentally evaluated in terms of the edge spread function (ESF). ESF was determined following a procedure modified from the classical method used in MRI [35] and from the work of Halpern's group,[36–38] as previously published by our laboratory.[27,39] Briefly, a parallelepiped phantom made of AmFo or LiFo was homogeneously irradiated (300 Gy) with an external 250 kVp x-ray beam. The size of the phantom was $1.0\times1.0\times4.0$ (cm). A 2D image of the phantom was reconstructed. The image was acquired at 300 mT/m. The signal along a line perpendicular to the edge of the phantom was extracted from the image and the derivative was calculated. A nine-point smoothing algorithm was used to obtain the derivative curve, which was then fitted by a Gaussian function,

$$f(x) = \frac{1}{\sigma\sqrt{2\pi}} e^{-(x-\mu)^2/2\sigma^2}. \tag{2}$$

From the computed σ values, the full width at half maximum (FWHM) of the Gaussian curve was calculated from the following equation:

$$\mathrm{FWHM} = 2\cdot\sigma\sqrt{2\cdot\ln 2}. \tag{3}$$

All calculations and fitting were carried out using Prism 4 from GraphPad Software, Inc. (La Jolla, CA).

II.E. Gafchromic film dosimetry

Additional experimental measurements were performed using Gafchromic EBT films. Gafchromic EBT film (International Specialty Products, Wayne, NJ) sheets were cut into 2.2×2.2 (cm) squares. The calibration data set was obtained by exposing films at the following dose levels: 0, 1, 2, 4, 6, and 8 Gy with a 250 kVp x-ray beam using a 7×7 (cm) field size at a source surface distance of 33.5 mm.[15,40,41] EBT film was placed on top of a Plexiglas phantom during irradiations in full scatter conditions [phantom size of $30\times3\times30$ (cm)]. The effective measurement points were assumed to be at the center of the active emulsion layer, hence at 0.02 mm (half thickness of the active layer). EBT

films were selected because of their weak energy dependence dose response in the 50 kVp–10 MVp x-ray range.[40]

One set of EBT films was not irradiated to provide a background reading. EBT films were scanned in the portrait direction using a Vidar film scanner 2 h after irradiation to allow the saturation of color growth, according to the recommendations of the manufacturer, and processed using a dosimetry film software VXR-16 Dosimetry Pro. The pixel intensity (gray level) of exposed films was acquired with the software. The radial dose profiles were expressed as doses to the film and determined from EBT film data in 0.36 mm steps (the spatial resolution of the Vidar scanner). The films were also scanned at 7 days to verify postirradiation color stability over time. No significant variation was observed between both readings, a result that is consistent with that previously published data.[42]

For brachytherapy dosimetry, EBT films were placed between two ammonium formate phantoms of equal size (22.0 mm in diameter, 4.9 mm thick) and stacked together to prevent any air gap between them. A hole (0.4 mm in diameter) was drilled at the center of the films for the insertion of ^{192}Ir wires. A scheme of the experimental setup is shown in Fig. 1(b). Different exposure times (5, 20, and 30 min; 1, 2, and 18 h) were used in our experiments to prevent saturation at short radial distances. Each exposure was designed to measure the radial dose distribution for distances between 1.0 and 4.0 mm from the center of the source. The exposed films were digitized and analyzed as described above. The films were always digitized in the same orientation and read at the same time.

II.F. Monte Carlo calculations

The MCNP4C2 Monte Carlo code (Los Alamos, National Laboratory, USA)was used in this work. The code is utilized to model ^{192}Ir wires with surrounding geometry,[43] and the materials used in the MC calculations and their composition, density, and effective atomic number are presented in Table I. The photon interaction cross-section file used in this study was the DLC-200 library. The dose distribution (expressed as dose to ammonium formate) was calculated for short radial distances using the MC software code. A total of three different simulations was performed to provide comparisons with real measurements.

A first calculation was made for comparison with the EPRI results. The ^{192}Ir wires were modeled as cylinders with an inner cylindrical core of 0.1 mm in diameter encased in a 0.1 mm Pt cylindrical sheath with the same height. Cylindrical cells in the phantom were modeled with the same geometry as that used in the EPRI postprocessing. The radial dose distributions were modeled by placing concentric cylinders around the ^{192}Ir core and Pt encapsulation in 0.1 mm radial increments up to the 11 mm radius phantom.

The second simulation was performed for comparison with EBT film experimental data, including modeling of Gafchromic EBT films, placed between two cylindrical ammonium formate phantoms of equal size. Gafchromic EBT films were modeled for radial symmetry by placing concentric rings (0.234 mm high and with a thickness of 0.1 mm) around the wire source in the middle of phantoms. The energy deposition of the particles was scored within all films. We calculated the dose deposition using MC simulations for phantoms with or without insertion of Gafchromic EBT film. The insertion of EBT film did not affect the radial dose distribution.

TABLE I. The materials used in the Monte Carlo calculations and their composition, density, and effective atomic number.

Material	Element	Composition (% by weight)	Density (g/cm^3)	Z_{eff}
Ir	⋯	⋯	22.39	77
Pt	⋯	⋯	21.41	78
Ir(20%)	Ir	20	21.613	78
Pt(80%)	Pt	80	⋯	⋯
Air (dry)			0.001205	8
	C	0.0124	⋯	⋯
	N	75.5267	⋯	⋯
	O	23.1781	⋯	⋯
	Ar	1.2827	⋯	⋯
Ammonium formate			1.26	7.03
	N	22.21	⋯	⋯
	C	19.05	⋯	⋯
	H_5	7.99	⋯	⋯
	O_2	50.75	⋯	⋯
EBT film			1.1	6.98
	H	39.7	⋯	⋯
	C	42.3	⋯	⋯
	O	16.2	⋯	⋯
	N	1.1	⋯	⋯
	Li	0.3	⋯	⋯
	Cl	0.3	⋯	⋯

Finally, the third simulation was implemented, where the energy deposited in the medium was scored within the cylindrical rings with a thickness of 0.1 mm and a height of 1.0 mm along the longitudinal axis of the source. Photon doses were calculated from 0.3 to 11.0 mm from the source center in the radial direction, in 0.1 mm increments. In the longitudinal direction, 1 mm intervals were scored from the center of the source to 5.0 mm. It was observed that the dose gradients obtained from the two planes of different thicknesses were almost superimposed.

*F*6 tallies were employed for gamma calculations, measuring the photon track length traversing a voxel. The cutoff energy for photons was set at 10 keV [5] and used a minimum of 1×10^8 histories, which yielded the average standard error of 1% for all radial distances for the cases with and without the secondary electrons from Pt encapsulation.

III. RESULTS

Each reconstructed 2D EPR image reflected the known shape of phantoms. The color code directly depicts the radial dose distribution around the radioactive wire source, as shown in Fig. 1(c). The EPR signal intensity increased linearly with the delivered dose, as previously observed by others.[20,22]

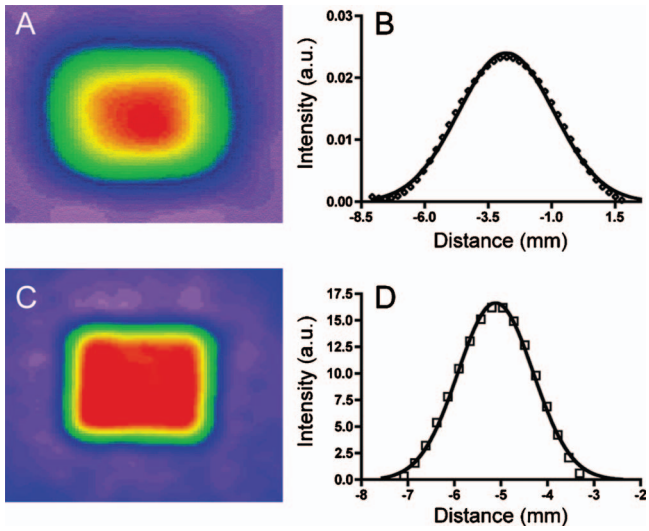

FIG. 2. Calculation of the edge spread function for the determination of the spatial resolution. (a) 2D EPR image of a square phantom made of LiFo and (b) ESF (diamonds) derived from the image and the fitted Gaussian curve. (c) 2D EPRI image for AmFo phantom. (d) ESF (boxes) and the corresponding fitted Gaussian curve.

Figure 2 shows the spatial resolution improvement due to ammonium formate at 300 mT/m. For lithium formate, the σ value computed from the Gaussian fit of ESF was 1.86 ± 0.03 with a corresponding resolution (FWHM) of 4.4 mm. The σ value for ammonium formate was 0.81 ± 0.02 and the computed resolution (FWHM) was 1.9 mm. The theoretical values were 4.6 mm (AmFo) and 2.1 mm (LiFo), respectively. In other words, the experimental resolution was increased by a factor of 2.3 when using AmFo vs LiFo at a gradient of field of 300 mT/m. When ammonium formate was used at a higher value of gradient (450 mT/m), the resolution was further increased up to 1.4 mm.

Figure 3(a) shows the radial dose profile measured with Gafchromic EBT films, as the average of three sets of data taken across a radial line from the center of the source. The comparison with MC calculations is shown in Fig. 3(b).

The comparison of EPRI results using different types of deconvolution (Gaussian or Fermi–Dirac) with MC simulations is presented in Fig. 4. It can be observed that the dose profile obtained with Gaussian filtered deconvolution is closer to the MC profile than the Fermi–Dirac filtered curve.

With a cylindrical ^{192}Ir wire source, the radioactive material is uniformly distributed throughout the wire, and the relative dose distribution in-plane is comparable to the average relative dose distribution from all planes in a full phantom. The relative radial dose values in-plane and for full phantoms, using the MCNP4C2 software code, were almost superimposed, and the insertion of EBT film did not affect the radial dose distribution from Gafchromic EBT films (data not shown).

Figure 5 shows the comparisons of the radial dose profiles obtained with the three different methodologies (film, EPRI, and MC). At distances ranging from 1.0 to 2.9 mm from the center of the phantom, the results of the EPRI data were consistent to within 1% with those of Gafchromic EBT films and MC simulations. At distances from 2.9 to 4.0 mm, the radial dose values obtained by EPRI were about 4% lower than those determined by MC simulations and EBT film dosimetry.

IV. DISCUSSION

The present study explores the ability of EPRI to estimate the relative dose distribution from low dose rate brachytherapy ^{192}Ir wire sources. The dosimetric properties of ammonium formate were previously described by Lund, Vestad, and co-workers using EPR spectroscopy.[20–22,44] They pointed out a linear dose-response relationship and a low radiation energy dependence, which are very desirable properties. Moreover, the lineshape of the EPR spectrum was simple and narrow, a very favorable feature for EPR imaging.

We ourselves previously demonstrated that 2D EPRI could be useful to determine the steep dose gradient around the brachytherapy ^{125}I seeds.[27] In that previous study, LiFo was used as the dosimetric material. The main limitation of the method was a poor spatial resolution because of the large

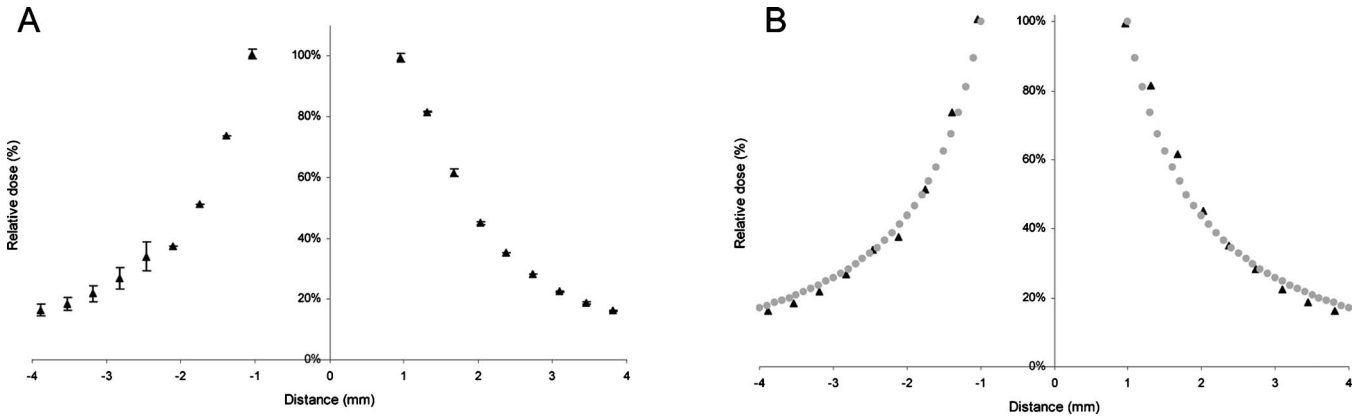

FIG. 3. (a) EBT film dosimetry profile using the setup presented in Fig. 1. The results are the average of three different data sets. Values are normalized at 1 mm from the center of the iridium wire. (b) Comparison of EBT film (black triangles) and Monte Carlo simulation (open squares) radial dose distributions for ammonium formate phantom irradiated by a ^{192}Ir wire source.

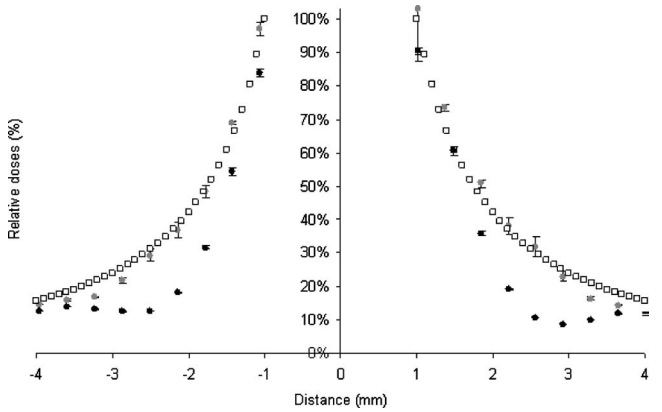

FIG. 4. Comparison of the Monte Carlo (open squares) and EPRI radial dose distributions obtained after Fermi–Dirac (black circles) or Gaussian (gray circles) deconvolution. EPR images were acquired with a gradient of field of 450 mT/m.

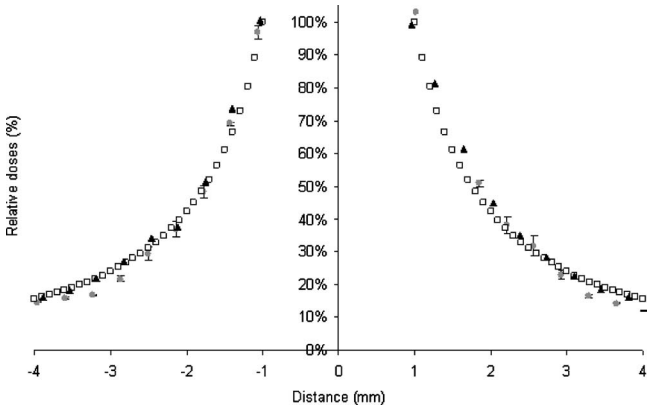

FIG. 5. Comparison of Monte Carlo (open squares), Gafchromic film (black triangles), and EPRI (gray circles) radial dose distributions for ammonium formate phantom irradiated by a ^{192}Ir wire source. Error bars for Gafchromic film are not plotted for more clarity but are available in Fig. 3(a).

linewidth (LW=1.4 mT) of LiFo. As the spatial resolution is inversely proportional to the EPR linewidth, in the present study, we investigated the possible usefulness of ammonium formate (LW=0.64 mT) as a dosimetric material in EPR imaging. The ultimate goal is to get reliable spatial dosimetric information, which is not achievable using EPR spectroscopy.

In the present work, we have demonstrated that it is possible to improve the spatial resolution by a factor of 2.3 using ammonium formate instead of lithium formate. We are now approaching a spatial resolution compatible with the range of dose distribution observed with brachytherapy sources.

Because of the relatively low signal-to-noise ratio in our EPR images, we found that a Gaussian filter was more adequate for the deconvolution process and gave results closer to the MC or film data than those obtained with Fermi–Dirac filtering. FD filtering uses a sharp cut-off frequency in the Fourier space, leading to theoretically sharper images, but it requires a very good signal with low noise. Gaussian filter is smoother and avoid high frequency artifacts with noisy data.

To verify the potential of EPRI as a tool to measure the dose distribution around brachytherapy ^{192}Ir wires, we compared this method to the theoretical Monte Carlo simulations and to the experimental data obtained with a standard reference method (film dosimetry). Our final results from the EPRI data were consistent within 1% with those from Gafchromic EBT films and MC simulations at short distances ranging from 1.0 to 2.9 mm from the center of the source. The radial dose values obtained by EPRI were lower by about 4% at distances from 2.9 to 4.0 mm than those determined by MC simulations and EBT film dosimetry. These differences can partially be explained by the presence of noise in the reconstructed 2D EPR images and by the still somewhat limited spatial resolution.

Because our data are normalized and expressed as relative doses, we can compare the profiles obtained with the three methodologies. The energy dependence of the dosimeters used can be quite different, but as our data are normalized, the effect of the energy dependence vanishes and comparisons are possible without further correction. Nevertheless, it must be mentioned that this energy effect will be of major importance for absolute dosimetry. Films and EPR dosimeters are calibrated according to the NCS dosimetry protocol[45] and are consequently expressed as dose to water. Monte Carlo simulations are computed as doses to dosimeter. For kV photons, a correction should be applied for the energy dependence of the dosimeter material. For high energy photons and electrons, the energy dependence is very low both for alanine and lithium formate.[46–50] Nevertheless, in the kV energy range, a substantial energy dependence has been demonstrated for alanine. A smaller dependence is observed for lithium formate[51] and ammonium formate,[22] so this point should be carefully investigated for future accurate absolute dosimetry.

We performed Monte Carlo simulations including different geometries. With a cylindrical ^{192}Ir wire source, the radioactive material is uniformly distributed throughout, and the relative dose distribution in-plane is comparable to the average relative dose distribution from all planes in a full phantom. The relative radial dose values in-plane and for full phantoms, using the MCNP4C2 software code, were almost superimposed, and the insertion of EBT film did not affect the radial dose distribution from Gafchromic EBT films.

This work provides a new experimental approach that completes the available range of techniques commonly used for dosimetry of low dose rate brachytherapy sources. They encompass theoretical Monte Carlo simulations[5,52] or experimental procedure such as MR Imaging using gel dosimeters,[53] optical detection with plastic scintillator[54] or solid polyurethane,[55] or even MOSFET dosimeter.[56]

V. CONCLUSIONS

Overall, ammonium formate is a suitable material, under certain conditions, for use in brachytherapy dosimetry and allows a marked improvement of the true spatial resolution achievable using EPRI. Nevertheless, it should be reminded that ammonium formate is a very hygroscopic material,

which limits its practical day-to-day use. In this study, we developed 2D EPRI dosimetry but 3D dosimetry is likely to be achieved with the EPRI approach in the future. Another interesting future perspective of the present study will be the development of absolute 2D and 3D quantification of the deposited absorbed doses.

ACKNOWLEDGMENTS

This study was supported by grants from the Belgian National Fund for Scientific Research (FNRS), the Télévie, the Fonds Joseph Maisin, the Saint-Luc Foundation, the Actions de Recherches Concertées–Communauté Française de Belgique (Grant No. ARC 09/14-020), and the Pôle d'Attraction Interuniversitaire PAI VI (Grant No. P6/38). The authors are grateful to Dr. Jean Marc Denis for his skillful assistance. The authors have no conflict of interest.

[a]Author to whom correspondence should be addressed. Electronic mail: bernard.gallez@uclouvain.be; Telephone: 32-2-7647391; Fax: 32-2-7647390.

[1]M. McJury, P. D. Tapper, V. P. Cosgrove, P. S. Murphy, S. Griffin, M. O. Leach, S. Webb, and M. Oldham, "Experimental 3D dosimetry around a high-dose-rate clinical ^{192}Ir source using a polyacrylamide gel (PAG) dosimeter," Phys. Med. Biol. **44**, 2431–2444 (1999).

[2]P. Karaiskos, P. Papagiannis, A. Angelopoulos, L. Sakelliou, D. Baltas, P. Sandilos, and L. Vlachos, "Dosimetry of ^{192}Ir wires for LDR interstitial brachytherapy following the AAPM TG-43 dosimetric formalism," Med. Phys. **28**, 156–166 (2001).

[3]R. Nath, H. Amols, C. Coffey, D. Duggan, S. Jani, Z. Li, M. Schell, C. Soares, J. Whiting, P. E. Cole, I. Crocker, and R. Schwartz, "Intravascular brachytherapy physics: Report of the AAPM Radiation Therapy Committee Task Group No. 60. American Association of Physicists in Medicine," Med. Phys. **26**, 119–152 (1999).

[4]R. Nath, L. L. Anderson, G. Luxton, K. A. Weaver, J. F. Williamson, and A. S. Meigooni, "Dosimetry of interstitial brachytherapy sources: Recommendations of the AAPM Radiation Therapy Committee Task Group No. 43. American Association of Physicists in Medicine," Med. Phys. **22**, 209–234 (1995).

[5]F. Ballester, C. Hernández, J. Pérez-Calatayud, and F. Lliso, "Monte Carlo calculation of dose rate distributions around ^{192}Ir wires," Med. Phys. **24**, 1221–1228 (1997).

[6]D. Baltas, P. Karaiskos, P. Papagiannis, L. Sakelliou, E. Loeffler, and N. Zamboglou, "Beta versus gamma dosimetry close to Ir-192 brachytherapy sources," Med. Phys. **28**, 1875–1882 (2001).

[7]N. Reynaert, M. Van Eijkeren, Y. Taeymans, and H. Thierens, "Dosimetry of ^{192}Ir sources used for endovascular brachytherapy," Phys. Med. Biol. **46**, 499–516 (2001).

[8]R. Wang and X. A. Li, "A Monte Carlo calculation of dosimetric parameters of ^{90}Sr/^{90}Y and ^{192}Ir SS sources for intravascular brachytherapy," Med. Phys. **27**, 2528–2535 (2000).

[9]J. F. Williamson and Z. Li, "Monte Carlo aided dosimetry of the microselectron pulsed and high dose-rate ^{192}Ir sources," Med. Phys. **22**, 809–819 (1995).

[10]J. C. Anctil, B. G. Clark, and C. J. Arsenault, "Experimental determination of dosimetry functions of Ir-192 sources," Med. Phys. **25**, 2279–2287 (1998).

[11]H. Tolli and K. A. Johansson, "Quality assurance in brachytherapy: The displacement effect in the vicinity of ^{60}Co and ^{192}Ir brachytherapy sources," Phys. Med. Biol. **38**, 1485–1492 (1993).

[12]R. K. Valicenti, A. S. Kirov, A. S. Meigooni, V. Mishra, R. K. Das, and J. F. Williamson, "Experimental validation of Monte Carlo dose calculations about a high-intensity Ir-192 source for pulsed dose-rate brachytherapy," Med. Phys. **22**, 821–829 (1995).

[13]S. T. Chiu-Tsao, T. L. Duckworth, N. S. Patel, J. Pisch, and L. B. Harrison, "Verification of Ir-192 near source dosimetry using GAFCHROMIC film," Med. Phys. **31**, 201–207 (2004).

[14]A. Niroomand-Rad, C. R. Blackwell, B. M. Coursey, K. P. Gall, J. M. Galvin, W. L. McLaughlin, A. S. Meigooni, R. Nath, J. E. Rodgers, and C. G. Soares, "Radiochromic film dosimetry: Recommendations of AAPM Radiation Therapy Committee Task Group 55. American Association of Physicists in Medicine," Med. Phys. **25**, 2093–2115 (1998).

[15]S. T. Chiu-Tsao, D. Medich, and J. Munro III, "The use of new GAFCHROMIC EBT film for ^{125}I seed dosimetry in Solid Water phantom," Med. Phys. **35**, 3787–3799 (2008).

[16]K. Mehta and R. Girzikowsky, "Alanine-ESR dosimetry for radiotherapy. IAEA experience," Appl. Radiat. Isot. **47**, 1189–1191 (1996).

[17]D. F. Regulla and U. Deffner, "Dosimetry by ESR spectroscopy of alanine," Int. J. Appl. Radiat. Isot. **33**, 1101–1114 (1982).

[18]R. B. Hayes, E. H. Haskell, A. Wieser, A. A. Romanyukha, B. L. Hardy, and J. K. Barrus, "Assessment of an alanine EPR dosimetry technique with enhanced precision and accuracy," Nucl. Instrum. Methods Phys. Res. A **440**, 453–461 (2000).

[19]L. Antonovic, H. Gustafsson, G. Alm Carlsson, and Å Carlsson Tedgren, "Evaluation of a lithium formate EPR dosimetry system for dose measurements around ^{192}Ir brachytherapy sources," Med. Phys. **36**, 2236–2247 (2009).

[20]H. Gustafsson, S. Olsson, A. Lund, and E. Lund, "Ammonium formate, a compound for sensitive EPR dosimetry," Radiat. Res. **161**, 464–470 (2004).

[21]A. Lund, S. Olsson, M. Bonora, E. Lund, and H. Gustafsson, "New materials for ESR dosimetry," Spectrochim. Acta, Part A **58**, 1301–1311 (2002).

[22]E. Lund, H. Gustafsson, M. Danilczuk, M. D. Sastry, A. Lund, T. A. Vestad, E. Malinen, E. O. Hole, and E. Sagstuen, "Formates and dithionates: Sensitive EPR-dosimeter materials for radiation therapy," Appl. Radiat. Isot. **62**, 317–324 (2005).

[23]Y. Morita, K. Ohno, K. Ohashi, and J. Sohma, "ESR imaging investigation on depth profiles of radicals in organic solid dosimetry," Int. J. Rad Appl. Instrum. [A] **40**, 1237–1242 (1989).

[24]S. Colacicchi, S. Onori, E. Petetti, and A. Sotgiu, "Application of low frequency EPR imaging to alanine dosimetry," Appl. Radiat. Isot. **44**, 391–395 (1993).

[25]M. Anton and H. J. Selbach, "Measurements of dose distribution in alanine using EPR imaging," Bruker Spin Report **157–158**, 48–51 (2006).

[26]H. Gustafsson, K. Kruczala, E. Lund, and S. Schlick, "Visualizing the dose distribution and linear energy transfer by 1D and 2D ESR imaging: A potassium dithionate dosimeter irradiated with C^{6+} and N^{7+} ions," J. Phys. Chem. B **112**, 8437–8442 (2008).

[27]E. S. Vanea, P. Leveque, F. Abboud, A. Bol, J. M. Denis, N. Kolbun, S. Vynckier, and B. Gallez, "Evaluation of the dose distribution gradient in the close vicinity of brachytherapy seeds using electron paramagnetic resonance imaging," Magn. Reson. Med. **61**, 1225–1231 (2009).

[28]P. Kuppusamy, M. Chzhan, and J. L. Zweier, *Principles of Imaging: Theory and Instrumentation*, Biological Magnetic Resonance Vol. 18 (Kluwer Academic/Plenum, New York, 2003), pp. 99–152.

[29]Y. C. Cheung *et al.*, "The dose distribution close to an ^{192}Ir wire source: EGS4 Monte Carlo calculations," Phys. Med. Biol. **42**, 401–406 (1997).

[30]Y. C. Cheung, P. K. N. Yu, E. C. M. Young, C. L. Chan, M. F. Ng, F. N. F. Tang, and T. P. Y. Wong, "The electron-dose distribution surrounding an ^{192}Ir wire brachytherapy source investigated using EGS4 simulations and GafChromic film," Appl. Radiat. Isot. **48**, 985–990 (1997).

[31]G. R. Eaton, S. S. Eaton, and K. Ohno, *EPR Imaging and In Vivo EPR* (CRC, Boca Raton, 1991).

[32]H. Fujii and L. J. Berliner, "One- and two-dimensional EPR imaging studies on phantoms and plant specimens," Magn. Reson. Med. **2**, 275–282 (1985).

[33]K. Ohno, "ESR imaging: A deconvolution method for hyperfine patterns," J. Magn. Reson. **50**, 145–150 (1982).

[34]A. Sotgiu *et al.*, "ESR imaging: Spatial deconvolution in the presence of an asymmetric hyperfine structure," J. Phys. C **20**, 6297 (1987).

[35]D. W. McRobbie, E. A. Moore, M. J. Graves, and M. R. Prince, *MRI. From Picture to Proton* (Cambridge University Press, Cambridge, 2003).

[36]K.-H. Ahn and H. J. Halpern, "Simulation of 4D spectral-spatial EPR images," J. Magn. Reson. **187**, 1–9 (2007).

[37]K.-H. Ahn and H. J. Halpern, "Object dependent sweep width reduction with spectral-spatial EPR imaging," J. Magn. Reson. **186**, 105–111 (2007).

[38]K.-H. Ahn and H. J. Halpern, "Spatially uniform sampling in 4-D EPR spectral-spatial imaging," J. Magn. Reson. **185**, 152–158 (2007).

[39]P. Levêque, Q. Godechal, A. Bol, F. Trompier, and B. Gallez, "X-band EPR imaging as a tool for gradient dose reconstruction in irradiated

bones," Med. Phys. **36**, 4223–4229 (2009).
[40]M. J. Butson, T. Cheung, and P. K. N. Yu, "Weak energy dependence of EBT gafchromic film dose response in the 50 kVp-10 MVp x-ray range," Appl. Radiat. Isot. **64**, 60–62 (2006).
[41]R. Hill, L. Holloway, and C. Baldock, "A dosimetric evaluation of water equivalent phantoms for kilovoltage x-ray beams," Phys. Med. Biol. **50**, N331–N344 (2005).
[42]T. Cheung, M. J. Butson, and P. K. Yu, "Post-irradiation colouration of Gafchromic EBT radiochromic film," Phys. Med. Biol. **50**, N281–N285 (2005).
[43]J. F. Briesmeister, MCNP—A general Monte Carlo N-particle transport code, Version 4C (Los Alamos National Laboratory, Los Alamos, 2000).
[44]T. A. Vestad, E. Malinen, A. Lund, E. O. Hole, and E. Sagstuen, "EPR dosimetric properties of formates," Appl. Radiat. Isot. **59**, 181–188 (2003).
[45]T. Grimbergen, A. Aalbers, B. Mijnheer, J. Seuntjens, H. Thierens, J. Van Dam, F. Wittkamper, and J. Zoetelief, "Dosimetry of low and medium energy x-rays: A code of practice for use in radiotherapy and radiobiology," NCS Report No. 10, 1997.
[46]M. Anton, R. P. Kapsch, M. Krystek, and F. Renner, "Response of the alanine/ESR dosimetry system to MV x-rays relative to (60)Co radiation," Phys. Med. Biol. **53**, 2753–2770 (2008).
[47]E. S. Bergstrand, H. Bjerke, and E. O. Hole, "An experimental investigation of the electron energy dependence of the EPR alanine dosimetry system," Radiat. Meas. **39**, 21–28 (2005).
[48]E. S. Bergstrand, K. R. Shortt, C. K. Ross, and E. O. Hole, "An investigation of the photon energy dependence of the EPR alanine dosimetry system," Phys. Med. Biol. **48**, 1753–1771 (2003).
[49]E. Malinen, E. Waldeland, E. O. Hole, and E. Sagstuen, "The energy dependence of lithium formate EPR dosimeters for clinical electron beams," Phys. Med. Biol. **52**, 4361–4369 (2007).
[50]G. G. Zeng, M. R. McEwen, D. W. Rogers, and N. V. Klassen, "An experimental and Monte Carlo investigation of the energy dependence of alanine/EPR dosimetry: II. Clinical electron beams," Phys. Med. Biol. **50**, 1119–1129 (2005).
[51]E. Waldeland, E. O. Hole, E. Sagstuen, and E. Malinen, "The energy dependence of lithium formate and alanine EPR dosimeters for medium energy x rays," Med. Phys. **37**, 3569–3576 (2010).
[52]R. van der Laarse, D. Granero, J. Perez-Calatayud, A. S. Meigooni, and F. Ballester, "Dosimetric characterization of Ir-192 LDR elongated sources," Med. Phys. **35**, 1154–1161 (2008).
[53]Y. De Deene, N. Reynaert, and C. De Wagter, "On the accuracy of monomer/polymer gel dosimetry in the proximity of a high-dose-rate ^{192}Ir source," Phys. Med. Biol. **46**, 2801–2825 (2001).
[54]M. Ishikawa, G. Bengua, K. L. Sutherland, J. Hiratsuka, N. Katoh, S. Shimizu, H. Aoyama, K. Fujita, R. Yamazaki, K. Horita, and H. Shirato, "A feasibility study of novel plastic scintillation dosimetry with pulse-counting mode," Phys. Med. Biol. **54**, 2079–2092 (2009).
[55]P. Wai, J. Adamovics, N. Krstajic, A. Ismail, A. Nisbet, and S. Doran, "Dosimetry of the microSelectron-HDR Ir-192 source using PRESAGE and optical CT," Appl. Radiat. Isot. **67**, 419–422 (2009).
[56]W. C. Toye, K. R. Das, S. P. Todd, M. B. Kenny, RR. D. Franich, and P. N. Johnston, "An experimental MOSFET approach to characterize ^{192}Ir HDR source anisotropy," Phys. Med. Biol. **52**, 5329–5339 (2007).